



Creep and stress relaxation behavior for natural cellulose crystal of wood cell wall under uniaxial tensile stress in the fiber direction

Takahisa Nakai¹ · Keisuke Toba² · Hiroyuki Yamamoto³

Received: 23 March 2018 / Accepted: 22 August 2018 / Published online: 17 November 2018
© The Author(s) 2018

Abstract

We investigated the temporal changes in creep and stress relaxation behavior in both microscopic crystalline cellulose and macroscopic strain of wood specimen using Japanese cypress (*Chamaecyparis obtusa* Endl.) to understand the viscoelastic properties of wood cell walls. Specimens 600 μm in thickness were observed by the X-ray diffraction and submitted to tensile load. The crystal lattice strain of (004) plane and macroscopic strain of specimen were continuously detected during creep and stress relaxation tests. It was found that the creep compliance based on macroscopic strain showed a gradual increase after instantaneous deformation due to loading and then the parts of creep deformation remained as permanent strain after unloading. On the other hand, crystal lattice strain showed a different behavior for macroscopic strain; it kept a constant value after instantaneous deformation due to loading and then increased gradually after a certain period of time. These differences between macroscopic and microscopic levels were never found in the stress relaxation tests in this study. Relaxation modulus at the macroscopic level only showed a decreasing trend throughout the relaxation process. However crystal lattice strain kept a constant value during the macroscopic relaxation process. In addition, the microfibril angle (MFA) of wood cell wall has a role of mechanical behavior at microscopic level; crystal lattice strains were smaller with increasing MFA at both creep and relaxation processes. Creep compliance and stress relaxation modulus at the macroscopic level decreased and increased with increasing MFA, respectively. Our results on the viscoelastic behavior at microscopic level evidenced its dependency on MFA.

Keywords Crystalline cellulose · Peak of (004) reflection · X-ray diffraction method · Viscoelastic properties · Cellulose microfibril angle

Introduction

Natural cellulose often forms a rigid crystal of microfibrils in wood cell walls. Its framework accounts for the majority of the cell walls. Especially in the middle layer of secondary walls, they align relatively parallel to the fiber direction. This structure is considered to contribute to the better mechanical properties of wood in longitudinal direction [1, 2].

It is well known that X-ray diffraction (XRD) techniques provide valuable information about molecular conditions of crystalline cellulose in wood cell walls (e.g., microfibril angle (MFA) [3, 4], crystallinity [5–7], crystal lattice spacing [8–13]). Some researchers found a relationship between stress loading in the longitudinal direction of wood and changes in the crystal lattice spacing [11, 12, 14–19]. In our previous work, we tried to investigate the relationship between changes in the crystal lattice strain of (004) plane and the longitudinal macroscopic strain of Japanese cypress (*Chamaecyparis obtusa* Endl.) under cyclic tensile stress [19]. It was found that the crystal lattice strain was always smaller than the macroscopic strain, regardless of the cyclic loading. Moriizumi and Okano [17] also found a similar relationship under some conditions of moisture content. They also investigated crystal lattice strains during creep and stress relaxation and proposed a mechanical model based on a series of crystalline

✉ Takahisa Nakai
jaja@bio.mie-u.ac.jp

¹ Graduate School of Bioresources, Mie University,
Tsu 514-8507, Japan

² Forestry and Forest Products Research Institute,
Tsukuba 305-8687, Japan

³ Graduate School of Bio-agricultural Science, Nagoya
University, Nagoya 464-8601, Japan

and amorphous substances. Zabler et al. [11] tried to understand the changes in crystal lattice spacing in (004), (200), (110), and (1 $\bar{1}$ 0) plane of crystalline cellulose in spruce (*Picea abies*) cell walls under stress loading during continuous moisture adsorption and desorption using synchrotron radiation techniques.

Indeed, the mixed structure of rigid crystal and amorphous regions like in wood cell walls often makes it complex to understand the relationship between wood strain and microscopic strain in cellulose molecular chains during stress loading. Therefore, more information based on additional and precise case studies are required to understand the mechanical behavior or spatial configuration of wood cell walls at microscopic level.

The purpose of this study is to investigate the effect of MFA of wood cell walls on the creep and relaxation process from the viewpoint of both microscopic and macroscopic levels. Thus, we collected detailed information of wood cell walls using XRD techniques under continuous longitudinal loading and unstressed condition.

Theory

The crystal lattice strain was obtained based on the Bragg's equation, as follows:

$$n\lambda = 2\bar{d} \sin \theta, \quad (1)$$

where \bar{d} is the crystal lattice spacing (nm) for each diffraction plane, λ is the incident X-ray wavelength (0.1542 nm), and θ is the Bragg angle ($^\circ$) for each plane on the basis of the peak position obtained by the X-ray diffraction diagram. In this study, $\Delta\bar{d}$ is regarded as a result of loading on a wood specimen, as well as the corresponding diffraction peak angle of incident X-ray ($\Delta\theta$) varying with it. Then, following equation is obtained when \bar{d} and θ are replaced by $\bar{d} + \Delta\bar{d}$ and $\theta + \Delta\theta$, respectively.

$$n\lambda = 2(\bar{d} + \Delta\bar{d}) \sin(\theta + \Delta\theta). \quad (2)$$

The Eq. (2) is expanded, as follows:

$$n\lambda = 2(\bar{d} + \Delta\bar{d}) \left\{ \sin \theta + \cos \theta \cdot \Delta\theta - \frac{1}{2} \sin \theta (\Delta\theta)^2 + \dots \right\}. \quad (3)$$

When the high-ordered terms $(\Delta\theta)^2$ and $\Delta\theta \cdot \Delta\bar{d}$ are ignored, we obtained:

$$n\lambda = 2\bar{d} \sin \theta + 2\bar{d} \cos \theta \cdot \Delta\theta + 2 \sin \theta \cdot \Delta\bar{d}. \quad (4)$$

Combining (1) and (4) yields:

$$\frac{\Delta\bar{d}}{\bar{d}} = -\cot \theta \cdot \Delta\theta. \quad (5)$$

Therefore, the crystal lattice strain can be calculated by substituting the declination of peak angle value of diffraction intensity before and after stress loading.

Experimental

Materials

The test specimens were prepared from Japanese cypress (*Chamaecyparis obtusa* Endl.). Average values of air-dried density, width of annual ring, and moisture content were 0.33 g/cm³, 1.5 mm, and 12%, respectively. The MFA of wood specimens were in the range of 9–21 $^\circ$. The crystallinity calculated from Segal method [20] was 54%. The dimensions and shape of test specimen were the same as in our previous study [18, 19]; quarter-sawn specimens with dimensions of 600 μm \times 10 mm \times 60 mm (R \times T \times L) were used. The middle part of all specimens was sawn to make dumbbell shape, and pieces of beech wood were glued on both edges of specimen using epoxy resin as a reinforcement material. A hole 5 mm in diameter was drilled at both ends to allow the bolt fixing on the tensile load attachment in XRD device. A strain gauge (gauge length: 5 mm, Tokyo Measuring Instruments Laboratory Co., Ltd., Japan) was pasted on the surface of center part using cyanoacrylate adhesive.

X-ray stress measurement

The tensile load attachment was mounted on the turntable of a goniometer according to the same method as our previous work [18, 19]. The tensile load, controlled by a desktop-type material testing machine, was applied parallel to the fiber direction through a stainless wire. An X-ray diffractometer (XD-D1w, Shimadzu Co., Japan) was used to measure the crystal lattice spacing of crystalline cellulose in wood cell walls under the following conditions. All XRD measurements were made with the transmission method. The incident X-ray radiation was a Cu K α characteristic X-ray passing through a nickel filter with a power of 40 kV and 40 mA. Both the air-scattering prevention slit and the divergence slit were 1 $^\circ$. The width of the detection slit was 0.1 mm. Continuous scanning was made with the driving shaft of $\theta - 2\theta$. Scanning speed and integration time were 0.125 $^\circ$ /min and 4.0 s, respectively. The diffraction intensity profile of the peak of (004) plane was measured in the range of $2\theta = 32.5\text{--}36.5^\circ$. The determination of diffraction peak angle was made using Gaussian approximation.

The load during tensile creep test and tensile stress relaxation test was determined based on the following

procedure. First, 10 specimens with the dimensions mentioned above were subjected to a static tensile test; 60% of the load at the proportional limit was adopted as the constant load ($\sigma_0 \approx 33.7$ MPa) in the tensile creep test. This load corresponding to a longitudinal stress of σ_0 was also adopted as the initial load of tensile stress relaxation test. Tensile load in stress relaxation test was gradually decreased to keep a constant macroscopic strain of specimen with the progress of stress relaxation. Three specimens were subjected to each X-ray stress measurement in this study.

All measurements were performed in the experimental laboratory where the temperature and relative humidity were kept at 20 °C (± 0.5 °C) and 60% ($\pm 1\%$), respectively. Control regulation of X-ray diffractometer with the tensile load attachment was made by a personal computer. Output values from the load cell, which was set for tensile load attachment, and measured values of macroscopic strain from the strain gauge were collected by a data logger (DE-1200IF, San-ei Instruments, Ltd., Japan) and stored in the personal computer.

Results

Tensile creep properties

Temporal changes in creep response

Figure 1 shows the temporal change of macroscopic strain and of (004) crystal lattice strain, fitted as functions $\epsilon_s(t)$ and $\epsilon_c(t)$, respectively, for each specimen having a different MFA. The macroscopic creep compliance $J_s(t)$ was defined by the following formula:

$$J_s(t) = \begin{cases} J_0 & (t = 0) \\ \epsilon_s(t)/\sigma_0 & (0 < t < t_r) \end{cases}, \quad (6)$$

where J_0 is a glass compliance calculated by back extrapolating $\epsilon_s(t)$ to $t=0$, t_r is the unloading time and σ_0 is the loading stress. $\epsilon_s(t)$ for both MFAs gradually increased with elapsed time, then an instantaneous elastic recovery occurred, followed by creep recovery after unloading. A part of macroscopic strain was still remaining 30 min after unloading. The extent was similar in both specimens ($\epsilon = 0.02\text{--}0.03\%$). On the other hand, $\epsilon_c(t)$ for both MFAs remained constant after instantaneous elastic deformation due to loading. Then, it began to show a gradual increase after 70 min. Both specimens also expressed strain recovery like for $\epsilon_s(t)$ after unloading, however, little permanent strain remained in comparison with macroscopic strain. It was found that $\epsilon_s(t)$ was always larger than $\epsilon_c(t)$ almost throughout the creep process in both specimens. However, $\epsilon_s(t)$ and $\epsilon_c(t)$ almost

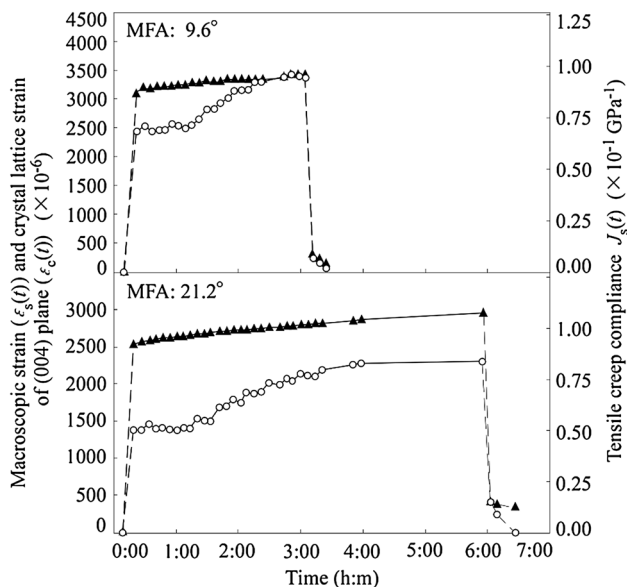


Fig. 1 Temporal changes in tensile creep response. $\epsilon_s(t)$; macroscopic strain (filled triangle), $\epsilon_c(t)$; crystal lattice strain of (004) plane (open circle), $J_s(t)$; ratio of macroscopic strain ($\epsilon_s(t)$) to constant stress ($\sigma_0 \approx 33.7$ MPa) (tensile creep compliance) (filled triangle)

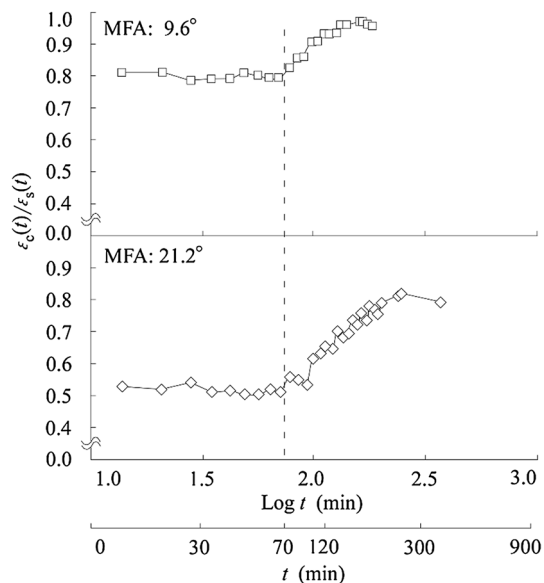


Fig. 2 Temporal changes in $\epsilon_c(t)/\epsilon_s(t)$ in tensile creep processes. Dashed line showed the elapsed time at $t = 70$ min

coincided each other in the specimen with small MFA at the latest stage of loading.

Relationship between $\epsilon_s(t)$ and $\epsilon_c(t)$

Figure 2 shows the relationship between $\epsilon_s(t)$ and $\epsilon_c(t)$. To analyze their relationship, the ratio of strains at each elapsed time ($\epsilon_c(t)/\epsilon_s(t)$), was plotted. It was found that the ratio kept almost a constant value and then began to increase after $\text{Log } t = 1.8$ ($t = 70$ (min.)) in both specimens. This means that the creep strains proceeded in the same degree at macroscopic and microscopic levels for the initial period ($t < 70$), and then the creep strain of crystal lattice began to significantly increase. This increasing trend of the ratio was expressed until the end of loading. Moreover, the ratio at 70 min was larger in the specimen with small MFAs.

Changes in the diffraction intensity in creep process

Figure 3 shows the ratio of diffraction intensity of (004) plane of crystalline cellulose $I(t)$ to its initial value (I_0). It was found that $I(t)/I_0$ slightly decreased, then seemed to increase around $\text{Log } t = 1.8$. A more significant effect was found in the specimen with large MFA (21.2°) compared to the smaller one. It was also found that $I(t)/I_0$ was smaller than 1.0 throughout the creep process.

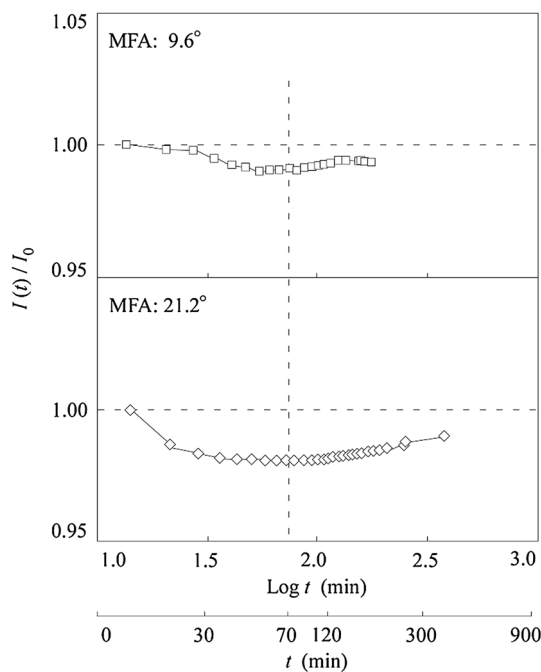


Fig. 3 Temporal changes in $I(t)/I_0$ in tensile creep processes. $I(t)$ and I_0 : diffraction intensities of (004) plane of crystalline cellulose in tensile creep process of wood specimens under the loaded and unloaded conditions, respectively

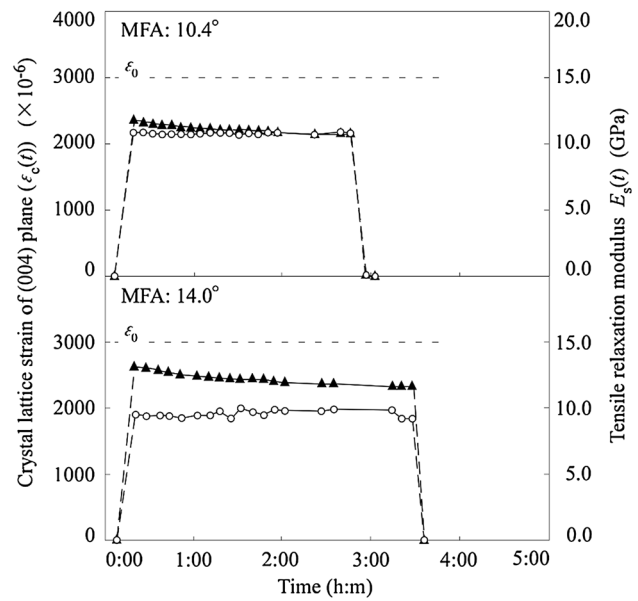


Fig. 4 Temporal changes in tensile relaxation response. $\epsilon_c(t)$; see legend in Fig. 1 (open circle), $E_s(t)$; ratio of stress to constant strain ($\epsilon_0 \approx 3000 \times 10^{-6}$) (tensile relaxation modulus) (filled triangle)

Tensile stress relaxation properties

Behaviors of relaxation response

Figure 4 shows the temporal change of crystal lattice strain $\epsilon_c(t)$, the imposed macroscopic strain ϵ_0 , and the macroscopic relaxation modulus defined as the ratio of loading stress $\sigma(t)$ to ϵ_0 according to the following formula:

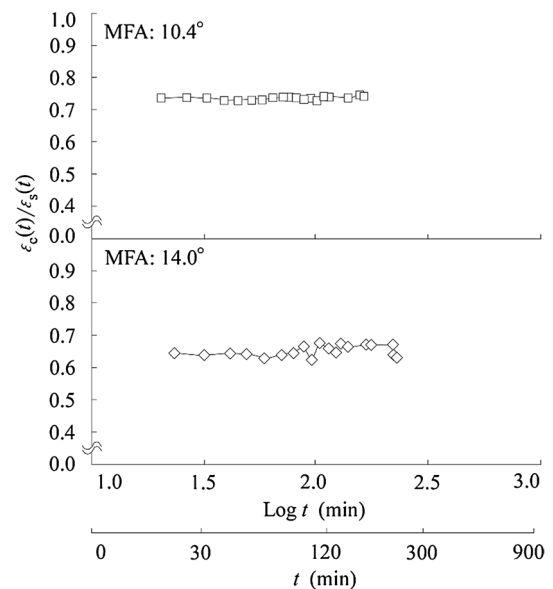


Fig. 5 Temporal changes in $\epsilon_c(t)/\epsilon_s(t)$ in tensile stress relaxation processes

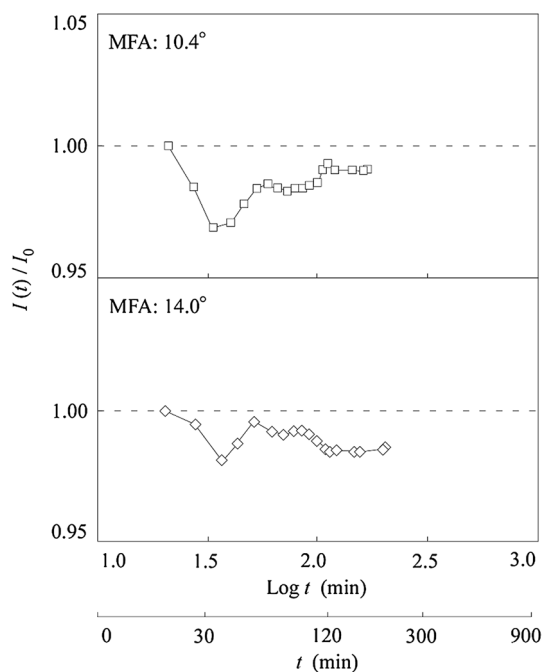


Fig. 6 Temporal changes in the value of $I(t)/I_0$ in tensile stress relaxation processes

$$E_s(t) = \begin{cases} E_0 & (t = 0) \\ \sigma(t)/\epsilon_0 & (0 < t < t_r) \end{cases}, \tag{7}$$

where E_0 is the static Young’s modulus calculated by back extrapolating $E_s(t)$ to $t=0$, t_r is the unloading time and ϵ_0 is a constant value. $E_s(t)$ for both MFAs gradually decreased with the progress of relaxation time. However, it recovered its initial value soon after unloading. Moreover, $\epsilon_c(t)$ in the specimen with small MFA (10.4°) was always larger than that with small MFA (14.0°).

Relationship between $\epsilon_s(t)$ and $\epsilon_c(t)$

Figure 5 shows the relationship between $\epsilon_s(t)$ ($= \epsilon_0$) and $\epsilon_c(t)$. The ratio remained almost constant for both MFAs throughout the stress relaxation processes unlike in the case of creep test.

Changes in the diffraction intensity in stress relaxation process

Figure 6 shows the ratio of the diffraction intensity of (004) plane of crystalline cellulose ($I(t)$) to that without loading (I_0). The values of $I(t)/I_0$ showed random variation below 1.0 throughout the stress relaxation test for both MFAs.

Discussion

The evaluation of strains in cellulose crystal lattice of (004) plane (functions $\epsilon_c(t)$) until unloading indicates a viscoelastic behavior at the microscopic level, dependent on MFA like in previous work [17]. Indeed, the obtained results suggest that $\epsilon_c(t)$ is dependent on the MFA; $\epsilon_c(t)$ decreases with increasing MFAs for both tensile creep and stress relaxation (Open circles in Figs. 1, 4). In our previous work, the wood cell walls with large MFAs under longitudinal tensile stress showed smaller deformation in the cellulose crystalline region than wood cell walls with small MFAs, while macroscopic strains in both specimens were of the same amount [18]. In other words, the smaller values of ϵ_c/ϵ_s were found in specimens with larger MFA. The values of $\epsilon_c(t)/\epsilon_s(t)$ in this study were 0.79 (MFA = 9.6°) and 0.52 (MFA = 21.2°) at $\text{Log } t = 1.8$ ($t = 70$ (min.)), while those were 0.74 (MFA = 10.4°) and 0.66 (MFA = 14.0°) throughout relaxation stress processes. This dependency on MFA is considered to coincide with our previous work [18]. Thus, it is considered that the increasing MFA prevents cellulose microfibril from stress loading parallel to the molecular chains in microscopic level, regardless of macroscopic deformations.

It is known that the changes in diffraction intensity are proportional to the changes in orientation of the target material, because the certain diffraction intensity in the reciprocal lattice space is proportional to the function of orientation distribution [21]. We hypothesized that the repeated tensile loading and unloading irreversibly induced a certain convergent value of MFA based on the results of our previous works [18, 19]. This hypothesis is supported by the tensile creep result shown in Fig. 3, although a clear trend was never observed in stress relaxation as shown in Fig. 6.

Previous studies proposed some models of native cellulose microfibrils including wood cell walls based on the combination of the ratio or special configuration of crystalline and amorphous substances [17, 22–26]. These models could conveniently express the overall mechanical properties of target materials. Indeed, a model consisting of an amorphous region of lignin and hemicellulose connected in parallel to a series of crystal and amorphous cellulose could well express the results of this study, if we daringly propose the most convenient and simple model. However, we consider that such model is effective in the case of polymer materials with a known molecular structure, but not in the case of wood cell walls where the microstructure remains unclear. The information of crystalline structure of native cellulose collected by XRD techniques is averaged, and the high-ordered structure of the wood cell wall must have a disarray between average and actual conditions. Therefore, we believe that it is essential to accumulate the common

recognition based on numerical measurement data of various mechanical phenomena both from macroscopic and microscopic viewpoints for grasping the whole picture of realistic microstructure of wood cell wall rather than seeking to understand them only based on the simple two-phase model of crystal and amorphous substances.

Open Access This article is distributed under the terms of the Creative Commons Attribution 4.0 International License (<http://creativecommons.org/licenses/by/4.0/>), which permits unrestricted use, distribution, and reproduction in any medium, provided you give appropriate credit to the original author(s) and the source, provide a link to the Creative Commons license, and indicate if changes were made.

References

- Cave ID (1969) The longitudinal Young's modulus of *Pinus radiata*. *Wood Sci Technol* 3:40–48
- Kojima Y, Yamamoto H (2004) Effect of microfibril angle on the longitudinal tensile creep behavior of wood. *J Wood Sci* 50:301–306
- Cave ID (1966) Theory of X-ray measurement of microfibril angle in wood. *For Prod J* 16:37–42
- Yamamoto H, Okuyama T, Yoshida M (1993) Method of determining the mean microfibril angle of wood over a wide range by the improved Cave's method. *Mokuzai Gakkaishi* 39:375–381
- Alexander LE (1969) X-ray diffraction in polymer science. Wiley, Amsterdam, pp 423–424
- Okano T (1970) Determination of crystallinity index of the wood by X-ray. *Mokuzai Gakkaishi* 16:257–261
- Toba K, Yamamoto H, Yoshida M (2013) Crystallization of cellulose microfibrils in wood cell wall by repeated dry-and-wet treatment, using X-ray diffraction technique. *Cellulose* 20:633–643
- Nishimura H, Okano T, Asano I (1981) Fine structure of wood cell walls 1. Structural features of noncrystalline substances in wood cell walls. *Mokuzai Gakkaishi* 27:611–617
- Sobue N, Shibata Y, Mizusawa T (1992) X-ray measurement of lattice strain of cellulose crystals during the shrinkage of wood in the longitudinal direction. *Mokuzai Gakkaishi* 38:336–341
- Hill SJ, Kirby NM, Mudie ST, Hawlay AM, Ingham B, Franich RA, Newman RH (2010) Effect of drying and rewetting of wood on cellulose molecular packing. *Holzforschung* 64:421–427
- Zabler S, Paris O, Burgert I, Fratzl P (2010) Moisture changes in the plant cell wall force cellulose crystallites to deform. *J Struct Biol* 171:133–141
- Montero C, Clair B, Alm eras T, van der Lee A, Gril J (2012) Relationship between wood elastic strain under bending and cellulose crystal strain. *Compos Sci Technol* 72:175–181
- Toba K, Yamamoto H, Yoshida M (2012) Mechanical interaction between cellulose microfibrils and matrix substances in wood cell walls induced by repeated wet-and-dry treatment. *Cellulose* 19:1405–1412
- Suzuki M (1968) Mechanical deformation of crystal lattice of cellulose in Hinoki wood. *Mokuzai Gakkaishi* 14:268–275
- Sobue N, Hirai N, Asano I (1971) On the measurement of strain distribution in wood under the axial tension force by X-ray diffraction. *Zairyu* 20:1188–1193
- Sobue N, Hirai N, Asano I (1971) Studies on structure of wood by X-ray II. Estimation of the orientation of micelles in cell wall (in Japanese). *Mokuzai Gakkaishi* 17:44
- Moriizumi S, Okano T (1978) Viscoelasticity and structure of wood 4. Behavior of crystal lattice strain depended on moisture content and time. *Mokuzai Gakkaishi* 24:1–6
- Nakai T, Yamamoto H, Nakao T (2005) The relationship between macroscopic strain and crystal lattice strain in wood under uniaxial stress in the fiber direction. *J Wood Sci* 51:193–194
- Nakai T, Yamamoto H, Nakao T, Hamatake M (2006) Mechanical behavior of the crystal lattice of natural cellulose in wood under repeated uniaxial tension stress in the fiber direction. *Wood Sci Technol* 40:683–695
- Segal L, Creely JJ, Martin AE, Conrad CM (1959) An empirical method for estimating the degree of crystallinity of native cellulose using the X-ray diffractometer. *Text Res J* 29:786–794
- Sobue N, Hirai N, Asano I (1971) Studies on structure of wood by X-ray 2. Estimation of the orientation of micells in cell wall. *Mokuzai Gakkaishi* 17:44–50
- Suzuki M (1969) Relationship between Young's modulus and the cell wall structures of sugi (*Cryptomeria japonica* D. Don). *Mokuzai Gakkaishi* 15:278–284
- Harada H (1982) Report for a grant-in-aid for scientific research (Japanese Ministry of Education) (in Japanese). *Science and Culture* (no. 57360010)
- Nishino T, Takano K, Nakamae K (1995) Elastic modulus of the crystalline regions of cellulose polymorphs. *J Polym Sci Part B* 33:1647–1651
- Ishikawa A, Okano T (1997) Fine structure and tension properties of ramie fibers in the crystalline form of cellulose I, II, III, and IV. *Polymer* 38:463–468
- Okano T (1999) Report for a grant-in-aid for scientific research (Japanese Ministry of Education) (in Japanese). *Science and Culture* (no. 08306009)